24th INTERNATIONAL CONGRESS ON SOUND AND VIBRATION
23–27 July 2017, London

RESONANCE-COUPLING EFFECT ON BROAD BAND GAP FORMATION AND SOUND ABSORPTION IN LOCALLY RESONANT SONIC METAMATERIALS WITH WOODPILE STRUCTURE

Wang Yuren

Key Laboratory of Microgravity, Institute of Mechanics, Chinese Academy of Sciences, Beijing, People's Republic of China
email: yurenwang@imech.ac.cn

Jiang Heng

Key Laboratory of Microgravity, Institute of Mechanics, Chinese Academy of Sciences, Beijing, People's Republic of China
email: hengjiang@imech.ac.cn

Chen Meng

Key Laboratory of Microgravity, Institute of Mechanics, Chinese Academy of Sciences, Beijing, People's Republic of China
email: chenmeng@imech.ac.cn

Guo Yanhong

College of Materials Science and Chemical Engineer, Harbin Engineering University, Harbin, People's Republic of China
email: guoyanhong@hrbeu.edu.cn

Sonic metamaterials have important applications in many fields such as noise control, and acoustic communication. Bwand gap and sound-absorbing spectrum are main judgements for the properties of sonic metamaterials. To broaden the resonant band gap and sound-absorbing spectrum, Woodpile structure was introduced into sonic metamaterials. Woodpile locally resonant sonic metamaterials (LRSMs) are formed by orthogonally stacking square coated-ultralight metal rods and embedding them layer by layer in an poly urethane (PU) matrix. Calculations suggest that Woodpile LRSMs have wider band gaps, which are adaptable to all types of vibration polarizations. Using vibration modes and a mass-spring model, strong coupling effect is confirmed between the orthogonal resonances at the upper edge of the band gap, providing a wider bandwidth. Moreover, considering viscoelasticity of materials, woodpile LRSMs can implement strong sound-absorbing effect in a wide range, which provides a new idea for the design and preparation of light weight and low frequency underwater sound-absorbing materials.
Keywords: Metamaterials, Band gap, Sound absorption, Woodpile structure, FEM

1. Introduction

Locally resonant sonic metamaterials (LRSMs) have attracted much attention for their ability to break through the mass density law and exhibit novel physical properties, such as a negative modulus, negative density and band gaps [1–5]. Typical LRSMs are made of distributed inclusions embedded in a hard matrix and have superiority in shielding low-frequency sound because of their sub-wavelength band gaps [6–10]. A key issue for the industrial application of an LRSM is the nar-

row bandwidth produced by the formation mechanism of the resonant band gap [11]. It has been found that relatively wide band gaps can be obtained by changing the LRSM structure [12–15] or by varying the elastic characteristics of the component materials [16–18]. However, these methods are usually based on changing intrinsic local resonance properties and thus usually limited and ineffective. Although the broadband effect of locally resonant sonic shields has been realized by combing resonances of different frequency, the manufacture of the shields is too complicated to be practical [11,16,19]. A novel LRSM is reported in this paper with the aim to use coupling resonances to broaden the band gap.

A natural idea has been proposed to broaden the bandwidth of LRSMs using the coupling effect of resonators. The coupling of resonators produces a new vibration mode that affects and widens the band structure [20-24]. However, in the case of LRSMs having traditional structure, such as two-dimensional LRSMs with rod dispersal [6,25–27] and three-dimensional LRSMs with sphere dispersal [1,7], the coupling effect between resonators has been rarely reported. In traditionally structured LRSMs, the unit cell usually contains one resonator, and the formation of the band gap depends on the vibrations of the isolated resonators. The vibration mode of the resonators at the lower edge of the band gap is the vibration of the scatterers considered as particles [1,28]. In contrast, the vibration mode of the resonators at the upper edge of the band gap is the relative vibration between the matrix and scatterers [1,28]. There is only a phase difference and no correlation between the resonators in adjacent lattices. Thus, the movements of resonators in traditionally structured LRSMs are usually isolated and coupling is too weak to be observed. It is thus recognized that the introduction of complex lattices that contain multiple resonators in one unit cell is needed for LRSMs to have strong coupling between resonators.

The present paper proposes a novel two-dimensional LRSM with complex lattices: a structure that is stacked layer-by-layer and having orthogonal resonations. Calculations suggest that there is strong coupling between the orthogonal resonations in the unit cell and that coupling produces a wider band gap for LRSMs with a woodpile structure. Compared with the two-dimensional LRSM having the same components, band gaps of woodpile-structure LRSMs adapt to all types of vibration polarization (i.e., longitudinal and transverse) and are wider by 128 Hz. In addition, considering viscoelasticity of materials, woodpile LRSMs can implement strong sound-absorbing effect in a wide range.

2. Model and method of calculation

The structure of a woodpile LRSM is shown in Figure 1b and its two-dimensional LRSM variant in Figure 1a. The woodpile structure can be obtained when the coated square column of the two-dimensional LRSM in the interval position is rotated 90 degrees. In the present study, the scatters are made of steel and the coating material is silicone rubber. Coated steel square columns were embedded in a matrix made of epoxy and the coupling effect was investigated by calculating the band gap structure and vibration modes.

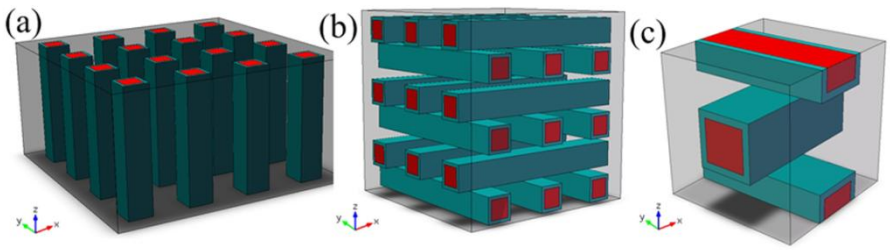

FIG. 1. Schematics of LRSMs: (a) a two-dimensional LRSM, (b) a stacked-structure LRSM, and (c) a unit cell of a woodpile structure with a simple cubic lattice.

Finite element methods (FEMs) are commonly used to calculate the band structure and vibration modes of LRSMs [29,30]. A distinct advantage of the FEM is the flexibility of modeling various materials with complex structure, good convergence and high precision [30]. The FEM software *COMSOL Multiphysics* was used to calculate the band structure and transmission. With an FEM based on the Bloch theorem, calculations of the dispersion relationship were made. The governing equation of elastic wave propagation in solids is given by

$$\rho \frac{\partial^2 u_i}{\partial t^2} = \sum_{j=1}^{3} \frac{\partial}{\partial x_j} \left(\sum_{l=1}^{3} \sum_{k=1}^{3} c_{ijkl} \frac{\partial u_k}{\partial x_l} \right), \qquad (i = 1,2,3), \tag{1}$$

where ρ is the density, u_i is the displacement, t is time, C_{ijkl} denotes elastic constants, and x_j denotes the coordinate variables x, y and z. Here, it is assumed that the displacement varies harmonically over time. Thus, the discrete form of eigenvalue equations of the FEM in the unit cell can be written as

$$(K - \omega^2 M)u = 0, \tag{2}$$

where K and M are respectively the stiffness and mass matrices, u is the displacement and ω is the angular frequency. According to the Bloch theorem, only one unit cell needs to be considered in the calculation.

The woodpile structure can be considered a simple cubic lattice. A schematic of a woodpile-structure unit cell with a simple cubic lattice is shown in Figure 1c. The structure is assumed to be infinite and periodic in the x, y and z directions. Because the calculation is compressed in one unit cell, the band structure is calculated by applying the Bloch–Floquet periodic boundary conditions for the boundaries of the unit cell along the x, y and z directions [31]:

$$\begin{aligned} u(x + a, y, z) &= u(x, y, z) e^{i(k_x \cdot a)}, \\ u(x, y + a, z) &= u(x, y, z) e^{i(k_y \cdot a)}, \\ u(x, y, z + a) &= u(x, y, z) e^{i(k_z \cdot a)}, \end{aligned} \tag{3}$$

where k_x, k_y and k_z are the components of the Bloch wave vector in the x, y and z directions respectively, and a is the lattice constant. With a given wave number k, a series of eigenfrequencies and corresponding eigenmodes can be obtained employing the FEM. The band structure can be obtained by sweeping k along the boundaries of the first Brillouin zone. The selected material parameters were density ρ = 1.18 g/cm^3, Young's modulus E = 435 MPa, and shear modulus G = 159 MPa for the epoxy background; ρ = 1.3 g/cm^3, E = 0.1175 MPa, and G = 0.04 MPa for the silicone rubber; and ρ = 7.78 g/cm^3, E= 201.6 GPa, and G = 81 GPa for the steel square columns.

The Acoustic-solid Interaction (frequency domain) module was used to calculate the transmission spectrum. Finite woodpile units are considered on the z axis, and infinite units along x and y axes are considered using Bloch–Floquet periodic boundary conditions. It was assumed that a plane sound wave is incident along the z axis and used transmission coefficients to represent the transmission spectrum of the woodpile-structure LRSM. To reduce reflection at boundaries, perfectly matched layers were chose to model infinite air domains at the top and bottom.

3. Results and discussion

The woodpile-structure LRSMs are transformed from two-dimensional LRSMs, and we thus discuss first the differences in their band structures. The band structures of the two-dimensional LRSM and woodpile-structure LRSM are shown in Figures 2 a and b, respectively. The width of the square rods is 0.3 cm. The thickness of the coating materials is 0.1 cm, and the lattice constant is 1 cm. For the two-dimensional structure, the displacement can be described by two independent parts: the pure transverse displacement along the z axis (dashed line in Fig. 2a) and the displacement of mixed longitudinal and transverse modes in the x, y plane (solid line in Fig. 2a). The band gap is between 1703.4 and 2227.9Hz for the modes in the x, y plane, and between 605.4 and 797.93 Hz for modes out of the x, y plane (as shown in Fig. 2a). Considering all types of vibration polarization (i.e., longitudinal and transverse), there are no absolute band gaps in the two-dimensional LRSM. For the woodpile structure, there is a band gap between 1758.9 and 2411.5 Hz. Owing to its three-

dimensional structure, the band gap adapts to all types of vibration polarization (as shown in Fig. 2b). The bandwidth of the woodpile-structure LRSM is approximately 652.6 Hz, which is approximately 128 Hz broader than that of the two-dimensional LRSM in the *x*, *y* plane. It is thus easier to realize a wider band gap that can be adapted to different polarization states with the woodpile-structure LRSM.

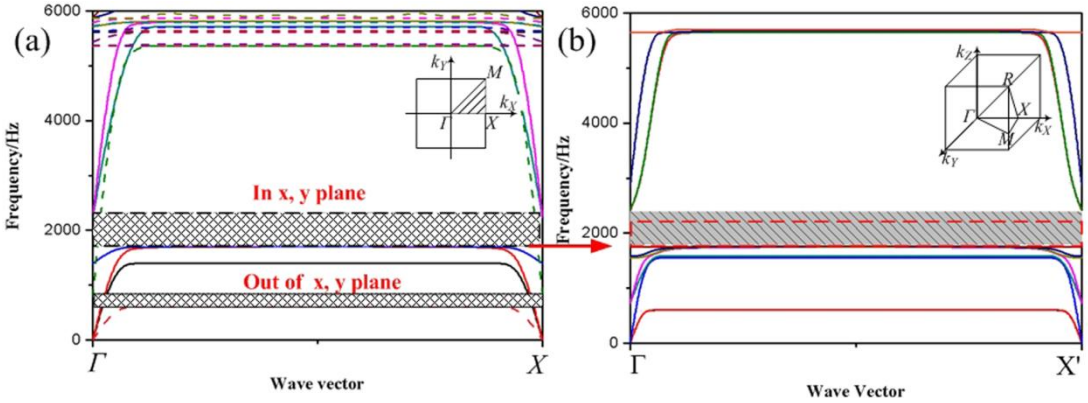

FIG. 2. Band structure of the two-dimensional LRSM (a) and stacked structure (b).

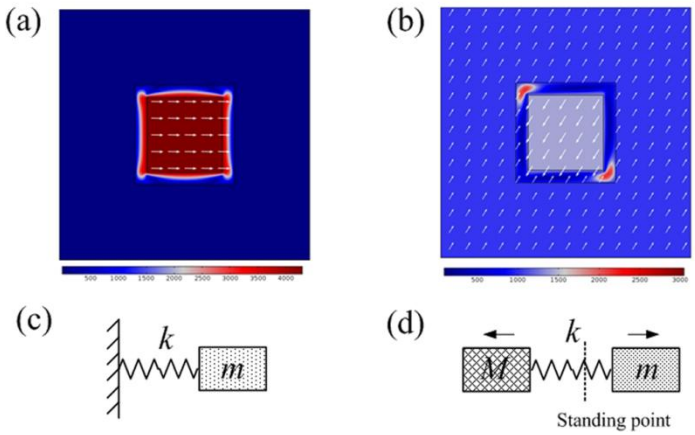

FIG. 3. Vibration modes and mass–spring models of the two-dimensional LRSM in the *x*, *y* plane: (a)(c) lower edge and (b)(d) upper edge of the band gap.

The vibration modes of lower and upper edges of band gaps in the *x*, *y* plane for the two-dimensional LRSM are shown in Figure 3a and b. It is seen that the vibration mode of the lower edge of the band gap is the vibration of a metal block considered as one particle, and a fixed delay in the phases of the vibrations between adjacent lattices maintains the dynamic balance of the whole system (Fig. 3a). [25,28] For the lower edge of the two-dimensional LRSM, the vibration model can be simplified as a mass–spring system (as shown in Fig. 3c), in which particle *m* represents the equivalent mass of the oscillator (steel block) and spring *k* represents the equivalent stiffness (of the coating material) of the oscillator. Additionally, the frequency of the lower edge can be evaluated as [32]

$$f_1 = \frac{1}{2\pi}\sqrt{\frac{k}{m}}. \tag{4}$$

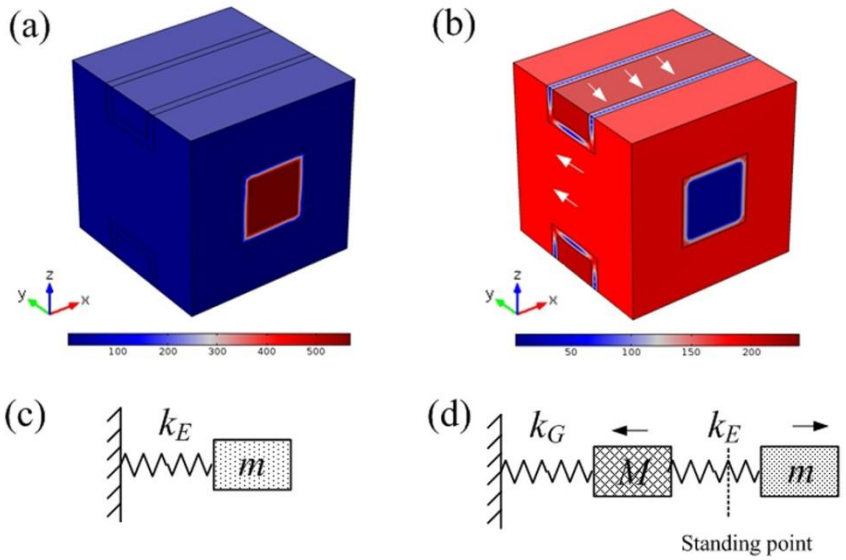

FIG. 4. Vibration modes and mass–spring models of the stacked-structure LRSM: (a)(c) lower edge and (b)(d) upper edge of the band gap.

In contrast, the vibration mode of the upper-edge band gap is the vibration of the host media with the reversed phase of the metal block (as shown in Fig. 3b) [24,27]. For the upper edge of the two-dimensional LRSM, the vibration model can be simplified as a mass–spring–mass system (as shown in Fig. 4b), in which particles m and M respectively represent the equivalent mass of the steel block and matrix, and spring k represents the equivalent stiffness of the coating material. The frequency of the lower edge can be evaluated as [32]

$$f_2 = \frac{1}{2\pi}\sqrt{\frac{k(m+M)}{mM}}. \tag{5}$$

The vibration modes at band gap edges out of the x, y plane are similar to those in the x, y plane, and their frequencies can also be evaluated with formulas (4) and (5). However, the value of the equivalent stiffness varies greatly between the two polarized modes. The compression or tension deformation produced by the tensile modulus of coating materials plays a dominant role in the x, y plane, and k is thus a function of tensile modulus E. Meanwhile, the shear deformation produced by the shear modulus dominates out of the x, y plane, and k is thus a function of shear modulus G. Because the tensile modulus is often greater than the shear modulus for common materials, frequencies of the band gap in the x, y plane are usually higher than those of out of the x, y plane, and it is difficult to overlap their band gaps in order to produce absolute band gaps for the two-dimensional LRSM. According to the vibration modes, the coupling between adjacent resonances is weak in the two-dimensional LRSM.

For the woodpile-structure LRSM, the vibration mode at the lower edge is the vibration of one steel column along the z axis, and the other columns are stationary relative to the matrix (Fig. 4a). We can make the same simplification of a mass–spring model in Figure 4c as made for the vibration mode of the two-dimensional LRSM in the x, y plane. The frequency is evaluated as

$$f_3 = \frac{1}{2\pi}\sqrt{\frac{k_E}{m}}, \tag{6}$$

where k_E is a function of tensile modulus E. The form of formula (6) is the same as that of formula (4), and the calculated frequency is similar to that of the lower edge of the two-dimensional LRSM.

The vibration mode of the upper-edge band gap (as shown in Fig. 3b) is one steel column perpendicular to the y direction vibrating with the matrix and the adjacent column parallel to the y direction being stationary. Two resonances exist in one unit cell at the upper-edge band gap: compression resonance (subject to the tensile modulus) and shear resonance (subject to the shear modulus). The compression resonance is the relative vibration between the vibrating column and matrix, and is similar to vibration of the two-dimensional LRSM in the x, y plane. Shear resonance is the vibra-

tion between the matrix and the stationary column, and is similar to vibration of the two-dimensional LRSM out of the *x*, *y* plane. We can simplify the vibration mode of the upper-edge band gap as a mass–spring–mass–spring model (Fig. 4d). We evaluate the upper-edge frequency as

$$f_4 = \frac{1}{2\pi}\sqrt{\frac{(mk_G+Mk_E+mk_E)+\sqrt{(mk_G+Mk_E+mk_E)^2-4k_Gk_E}}{2mM}}, \quad (7)$$

where k_G and k_E are respectively functions of shear modulus *G* and tensile modulus *E*. Both formulas (5) and (7) contain k_E, and the value of f_4 is higher than that of f_3, thus opening a band gap. In addition, compared with formula (5), formula (7) includes the effect of shear-deformation-induced shear resonance between the matrix and stationary column. It is observed here that the frequency shifts to a higher value and the band gap widens. The above analysis reveals that there is strong coupling between cross resonances at the upper-edge band gap of the woodpile-structure LRSM originating from the interaction between compression resonance and shear resonance. This strong coupling produces a band gap adaptable to all polarization states when the wave travels along the *z* axis. In addition, both shear and compression deformations appear in coupled resonances, and the frequency is thus higher and the band gap wider. It is seen that the coupling effect is beneficial to the formation of a wider band gap.

For other types of LRSMs with complex lattices, such as multicoaxial cylindrical LRSMs [26], although multi-scale resonators have been introduced into one unit cell, the result has been multiple band gaps and the band gaps have not obviously widened. This is because the resonators with different frequencies vibrate in the same plane, and it is thus difficult to generate strong coupling between the resonators. In the woodpile-structure LRSM, the resonators in one unit cell are intentionally arranged in perpendicular directions, and they have the same resonant frequencies. The orthogonal resonators act together at the same frequency, thus readily generating strong coupling. It is seen that the coupling strength is related to the arrangement of resonators in the unit cell.

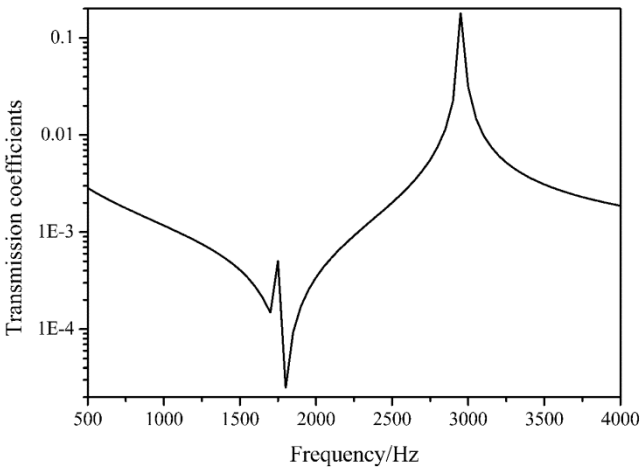

FIG. 5. Transmission coefficients of the stacked-structure LRSM in an air background.

The FEM was applied to investigate the transmission spectrum and better represent the band gap of the woodpile-structure LRSM. A plane sound wave in an air background is incident on a woodpile-structure LRSM having four units along the *z* axis and an infinite number along *x* and *y* axes. By sweeping the frequency, the transmission coefficients of the woodpile-structure LRSM in an air background were calculated as shown in Figure 5. It is seen that there are two peaks at 1750 and 2850 Hz, and a dip at 1850 Hz. The dip results from the band gap in which wave propagation is inhibited. The location of the dip agrees with the band gap region (1750 to 2400 Hz). The peaks are the result of resonances in which displacement along the *z* axis is dominant. The frequency of 1750 Hz is the lower band gap edge where the mass block vibration runs along the *z* axis and has the reverse phase in the adjacent unit cell, and thus couples with the sound wave traveling along the *z* axis to provide a magnified transmission coefficient. At 2850 Hz, although the frequency is not the edge

frequency of the band gap, the vibration mode is generated by the relative vibration of the matrix and steel column along the *z* axis. The transmission spectrum suggests that the woodpile-structure LRSM can be used as an acoustic filter or sound insulator.

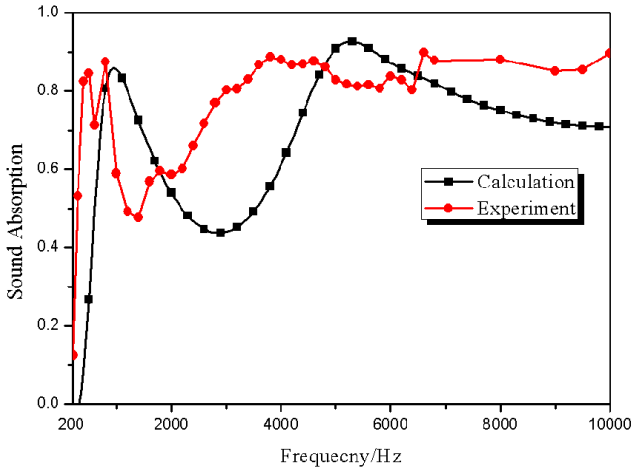

FIG. 6 Underwater absorption coefficients of the Woodpile structure LRSM

In LRSMs, locally resonant absorption coincides with viscoelastic deformation. Considering viscoelasticity of materials, woodpile LRSMs can implement strong sound-absorbing effect in a wide range (as shown in Fig. 6), which provides a new idea for the design and preparation of light weight and low frequency underwater sound-absorbing materials.

4. Conclusion

This study systematically investigated the band structures and vibration modes of woodpile-structure LRSMs to study coupling between resonances. The observed coupling produces a wider band gap that can be adapted to all types of vibration polarization. The calculated vibration modes and mass–spring model verify that strong coupling exists between orthogonal resonances (the shear resonance and compression resonance) at the upper edge of the band gap, and provides a wider bandwidth. In addition, considering viscoelasticity of materials, woodpile LRSMs can implement strong sound-absorbing effect in a wide range. The results suggest a novel design for broad band gaps, leading to further opportunities for practical applications of LRSM.

REFERENCES

1 Liu Z., Zhang X., Mao Y., Zhu Y., Yang Z., Chan C. T., and Sheng P., Locally resonant sonic materials, *Science* 289, 1734-1736 (2000).
2 Lai Y., Wu Y., Sheng P., and Zhang Z.Q., Hybrid elastic solids, *Nat. Mater*. **10**, 620-624 (2011).
3 Fang N., Xi D., Xu J., Ambati M., Srituravanich W., Sun C., and Zhang X., Ultrasonic metamaterials with negative modulus, *Nat. Mater*. **5**, 452-454 (2006).
4 Parnell W. J., Shearer T.. Antiplane elastic wave cloaking using metamaterials, homogenization and hyperelasticity. *Wave Motion*, , 50(7):1140–1152 (2013).
5 Titovich A. S., Norris A. N.. Tunable cylindrical shell as an element in acoustic metamaterial. *J. Acoust. Soc. Am.*, 136(4):1601-1609 (2014).
6 Liu Z., Chan C. T., and Sheng P., Three-component elastic wave band-gap material, *Phys. Rev. B* **65**, 165116 1-6 (2002).
7 Sheng P., Zhang X., Liu Z., and Chan C., Locally resonant sonic materials, *Physica B* **338**, 201-205 (2003).
8 Hirsekorn M., Small-size sonic crystals with strong attenuation bands in the audible frequency range, *Appl. Phys. Lett*. **84**, 3364-3366 (2004).
9 Zhao H., Liu Y., Wen J., Yu D. and Wen X., Tri-component phononic crystals for underwater anechoic coatings, *Phys. Lett. A* **367**, 224-232 (2007).

10 Hussein M. I., Leamy M. J., and Ruzzene M., Dynamics of Phononic Materials and Structures: Historical Origins, Recent Progress, and Future Outlook, *Appl. Mech. Rev*. 66, 040802 1-38 (2014).
11 Ho K. M., Cheng C. K., Yang Z., Zhang X., and Sheng P., Broadband locally resonant sonic shields, *Appl. Phys. Lett*. **83**, 5566-5568 (2003).
12 Zhang X., Liu Y., Wu F., and Liu Z., Large two-dimensional band gaps in three-component phononic crystals, *Phys. Lett. A* **317**, 144-149 (2003).
13 Gu Y., Luo X., and Ma H., Optimization of the local resonant sonic material by tuning the shape of the resonator, *J. Phys. D: Appl. Phys*. **41**., 205402 1-7 (2008).
14 Gu Y., Luo X., and Ma H., Low frequency elastic wave propagation in two dimensional locally resonant phononic crystal with asymmetric resonator, *J. Appl. Phys*. **105**, 044903 1-7 (2009).
15 Wang Y. F., Wang Y. S., and Wang L., Two-dimensional ternary locally resonant phononic crystals with a comblike coating, *J. Phys. D: Appl. Phys*. **47** 015502-015509 (2014),.
16 Liu Z., Yang S., and Zhao X., Chin. Ultrawide Bandgap Locally Resonant Sonic Materials, *Phys. Lett*. **22**, 3107-3110 (2005).
17 Lazarov B. S. and Jensen J. S., Low-frequency band gaps in chains with attached non-linear oscillators, *Int. J. Non-linear Mech*. **42**, 1186-1193 (2007).
18 Zhou X. and Chen C., Tuning the locally resonant phononic band structures of two-dimensional periodic electroactive composites, *Physica B* **431**, 23-31 (2013).
19 Meng H., Wen J., Zhao H., and Wen X., Optimization of locally resonant acoustic metamaterials on underwater sound absorption characteristics, *J. Sound Vib*. **331**, 4406-4416 (2012).
20 Xiao Y., Mace B. R., Wen J., and Wen X., Formation and coupling of band gaps in a locally resonant elastic system comprising a string with attached resonators, *Phys. Lett. A* **375**, 1485-1491 (2011).
21 Assouar M. B. and Oudich M., Dispersion curves of surface acoustic waves in a two-dimensional phononic crystal, *Appl. Phys. Lett.* **100**, 123506 1-3 (2012).
22 Assouar M. B., Sun J. H., Lin F. S., and Hsu J. C., Hybrid phononic crystal plates for lowering and widening acoustic band gaps, *Ultrasonics* **54**, 2159-2164 (2014).
23 Cheng Y., Xu J., and Liu X., Broad forbidden bands in parallel-coupled locally resonant ultrasonic metamaterials, *Appl. Phys. Lett*. 92, 051913 1-3 (2008).
24 Hladky-Hennion A. C., Allan G. and Billy M. D., Localized modes in a one-dimensional diatomic chain of coupled spheres, *J. Appl. Phys*. **98**, 054 909 1-7 (2005).
25 Zhao H., Liu Y., Wang G., Wen J., Yu D., Han X., and Wen X., Resonance modes and gap formation in a two-dimensional solid phononic crystal, *Phys. Rev. B* **72**, 012301 1-4 (2005).
26 Larabi H., Pennec Y., Djafari-Rouhani B., and Vasseur J. O., Multicoaxial cylindrical inclusions in locally resonant phononic crystals, *Phys. Rev. E* **75**, 066601 1-8 (2007).
27 Hirsekorn M., Delsanto P. P., Leung A. C., and Matic P., Elastic wave propagation in locally resonant sonic material: Comparison between local interaction simulation approach and modal analysis, *J. Appl. Phys*. **99**, 124912 1-8 (2006).
28 Liu Z., Chan C. T., and Sheng P., Analytic model of phononic crystals with local resonances, *Phys. Rev. B* **71**, 014103 1-8 (2005).
29 Wen J., Zhao H., Lv L., Yuan B., Wang G., and Wen X., Effects of locally resonant modes on underwater sound absorption in viscoelastic materials, *J. Acoust. Soc. Am*. **130**, 1201-1208 (2011).
30 Veres I. A., Berer T., and Matsuda O., Complex band structures of two dimensional phononic crystals: Analysis by the finite element method, *J. Appl. Phys*. **114**, 083519 1-11 (2013).
31 Oudich M., Li Y., Assouar B. M., and Hou Z., A sonic band gap based on the locally resonant phononic plates with stubs, *New J. Phys*. **12**, 083049 1-10 (2010).
32 Wang G., Shao L., Liu Y., and Wen J., Accurate evaluation of lowest band gaps in ternary locally resonant phononic crystals, *Chin. Phys*. **15**, 1843-184 (2006).